metals

MDPI

Article

Improved Dehydrogenation Properties of $2LiNH_2$-MgH_2 by Doping with Li_3AlH_6

Shujun Qiu [1], Xingyu Ma [1], Errui Wang [1], Hailiang Chu [1,2,*], Yongjin Zou [1], Cuili Xiang [1], Fen Xu [1] and Lixian Sun [1,*]

[1] Guangxi Key Laboratory of Information Materials, Guangxi Collaborative Innovation Center of Structure and Property for New Energy and Materials, School of Materials Science and Engineering, Guilin University of Electronic Technology, Guilin 541004, China; qiushujun@guet.edu.cn (S.Q.); maxingyuma@163.com (X.M.); Errui1990@163.com (E.W.); zouy@guet.edu.cn (Y.Z.); xiangcuili@guet.edu.cn (C.X.); xufen@guet.edu.cn (F.X.)

[2] Key Laboratory of Advanced Energy Materials Chemistry (Ministry of Education), Nankai University, Tianjin 300071, China

* Correspondence: chuhailiang@guet.edu.cn (H.C.); sunlx@guet.edu.cn (L.S.); Tel.: +86-773-2216607 (H.C. & L.S.); Fax: +86-773-2290129 (H.C. & L.S.)

Academic Editor: Jacques Huot
Received: 5 December 2016; Accepted: 23 January 2017; Published: 26 January 2017

Abstract: Doping with additives in a Li-Mg-N-H system has been regarded as one of the most effective methods of improving hydrogen storage properties. In this paper, we prepared Li_3AlH_6 and evaluated its effect on the dehydrogenation properties of $2LiNH_2$-MgH_2. Our studies show that doping with Li_3AlH_6 could effectively lower the dehydrogenation temperatures and increase the hydrogen content of $2LiNH_2$-MgH_2. For example, $2LiNH_2$-MgH_2-$0.1Li_3AlH_6$ can desorb 6.43 wt % of hydrogen upon heating to 300 °C, with the onset dehydrogenation temperature at 78 °C. Isothermal dehydrogenation testing indicated that $2LiNH_2$-MgH_2-$0.1Li_3AlH_6$ had superior dehydrogenation kinetics at low temperature. Moreover, the release of byproduct NH_3 was successfully suppressed. Measurement of the thermal diffusivity suggests that the enhanced dehydrogenation properties may be ascribed to the fact that doping with Li_3AlH_6 could improve the heat transfer for solid–solid reaction.

Keywords: hydrogen storage; Li-Mg-N-H system; Li_3AlH_6; thermal diffusivity; ball milling; phase transformation

1. Introduction

Safe and efficient storage of hydrogen is one of the major technological challenges associated with the use of hydrogen as an energy carrier, which is a vitally important process for the subsequent transition to the so called "hydrogen economy" [1]. Hydrogen can be stored as a compressed gas or as a cryogenic liquid; however, solid-state materials have the great potential to provide significantly high hydrogen storage densities, which draws a significant amount of research interest [2]. A long list of materials with a much higher hydrogen density have been synthesized and investigated during the past few decades. Several types of such materials mainly include microporous media that can physically adsorb hydrogen molecules at low temperatures [3], intermetallic hydrides that absorb atomic hydrogen as an interstitial, and complex hydrides that chemically absorb/desorb hydrogen [4,5]. Owing to the high hydrogen content, lightweight complex hydrides mostly containing Li, B, Na, Mg, and Al, such as alanates $[AlH_4]^-$, amides $[NH_2]^-$, amidoboranes $[NH_2BH_3]^-$, and borohydrides $[BH_4]^-$, are considered to be particularly promising as hydrogen storage materials [6–17]. The extensive studies of metal-N-H systems in recent years were initially prompted by Chen and coworkers, who

reported the absorption and desorption of hydrogen gas by lithium nitride (Li_3N) at high temperatures (195–255 °C) [18] according to Equation (1).

$$Li_3N + H_2 \leftrightarrow Li_2NH + LiH + H_2 \leftrightarrow LiNH_2 + 2LiH \quad (1)$$

The second step in Equation (1) with about 6.5 wt % of hydrogen was given much attention due to a fairly good reversibility. However, $LiNH_2$-LiH suffers from high operating temperatures and an emission of ammonia. To address these problems, the substitution of LiH by MgH_2 to form a $2LiNH_2$-MgH_2 system has a remarkable destabilization effect [19]. Complete dehydrogenation of the mixture of $2LiNH_2$-MgH_2 produces a new ternary imide of $Li_2Mg(NH)_2$, and the following rehydrogenation of $Li_2Mg(NH)_2$ is converted to a mixture of 2LiH-$Mg(NH_2)_2$ due to the thermodynamic stability. The whole reaction path can be expressed by Equation (2):

$$2LiNH_2 + MgH_2 \rightarrow Li_2Mg(NH)_2 + 2H_2 \leftrightarrow Mg(NH_2)_2 + 2LiH \quad (2)$$

Unfortunately, the dehydrogenation temperature of the $2LiNH_2$-MgH_2 system discussed above is still too high for practical applications (<100 °C) due to its high kinetic barriers. Many studies have been reported to focus on further altering the thermodynamics/kinetics of the $2LiNH_2$-MgH_2 system [20–23]. Doping with high-performance additives exhibits an excellent effect on reducing the temperature for hydrogen uptake and release. Lithium aluminum hydride ($LiAlH_4$) has a high hydrogen storage capacity (10.5 wt % H_2) and an excellent performance of hydrogen desorption at low temperature; thus, it has received significant attention from researchers. $LiAlH_4$ decomposes through a two-step process into Al, LiH, and H_2 at $T < 250$ °C through the intermediate Li_3AlH_6, according to reaction scheme (3) [24–29].

$$LiAlH_4 \rightarrow 1/3Li_3AlH_6 + 2/3Al + H_2 \rightarrow LiH + Al + 3/2H_2 \quad (3)$$

In particular, hexahydride of lithium alanate (Li_3AlH_6) releases hydrogen according to reaction (4) [13].

$$Li_3AlH_6 \rightarrow 3LiH + Al + 3/2H_2 \quad (4)$$

Hydrogen release from the $LiAlH_4$-$LiNH_2$ system was first reported by Xiong and coworkers [30]. It was found that $LiNH_2$ could effectively destabilize $LiAlH_4$ during the dehydrogenation process. The overall reaction of hydrogen release from this mixture was proposed as given by reaction (5).

$$LiAlH_4 + 2LiNH_2 \rightarrow Li_3AlN_2 + 4H_2 \quad (5)$$

Lu et al. [31] found that the reversible storage capacity of the Li_3AlH_6-$3LiNH_2$ system is increased to 7.0 wt % of hydrogen under 300 °C, according to the following reaction (6):

$$Li_3AlH_6 + 3LiNH_2 \leftrightarrow Al + 3Li_2NH + 9/2H_2 \quad (6)$$

The aforementioned reactions between lithium aluminum hydrides and lithium amide demonstrate the great potentials for the approach of destabilizing alanate materials with amides. In this study, the additives are focused on the catalytic enhancement of the dehydrogenation of $2LiNH_2$-MgH_2. We prepared Li_3AlH_6 and examined its effect on the hydrogen storage properties of $2LiNH_2$-MgH_2. The dehydrogenation properties and the thermal diffusivity of the combined system are discussed.

2. Materials and Methods

2.1. Sample Preparation

Li_3AlH_6 sample was prepared by mechanically milling LiH (95% purity, Sigma-Aldrich, St. Louis, MO, USA) and $LiAlH_4$ (95% purity, Sigma-Aldrich) in a molar ratio of 2:1 on a Retsch PM400 planetary

mill (Haan, Germany) at 200 rpm under 0.1 MPa of an argon atmosphere. The ball-to-powder weight ratio was set to about 30:1. $2LiNH_2$-MgH_2-XLi_3AlH_6 (X = 0, 0.05, 0.10, 0.15, and 0.20) composites were prepared by mechanically milling $LiNH_2$ (95% purity, Sigma-Aldrich) and MgH_2 (98% purity, Sigma-Aldrich) with and without Li_3AlH_6 additive. The ball-to-powder weight ratio was set to be about 60:1. To minimize the temperature increment of the samples during the ball milling process, there was a 30 s pause for each 2 min of milling. The total milling time was 20 h. All the sample handling was performed in an Ar-filled glove box, in which the typical H_2O/O_2 levels were below 1 ppm.

2.2. Structural Characterization and Property Evaluation

Temperature-programmed desorption (TPD) properties were measured on an automated chemisorption analyzer (ChemBet Pulsar TPD, Quantachrome, Boynton Beach, FL, USA). The sample was heated up to 300 °C at a rate of 5 °C/min in a reactor in flowing Ar gas. The temperature-dependence of hydrogen desorption was performed on a thermogravimetric apparatus (TG, SETSYS Evolution, SETARAM Instrumentation, Lyon, France)-mass spectrometer (MS, GAM 200, InProcess Instruments, Bremen, Germany) combined system to analyze the evolved gas composition. The sample was heated up to 300 °C at a rate of 5 °C/min in flowing Ar gas. The dehydrogenation capacity based on volumetric release was measured on a HyEnergy PCTPRO-2000 Sieverts-type apparatus (SETARAM Instrumentation, Lyon, France). Approximately 150 mg of sample powder was loaded into the sample holder and heated at 2 °C/min from room temperature to 300 °C initially under dynamic vacuum.

Structural identification of the phases in the samples at different stages was performed on a Bruker D8 Advance diffractometer (Cu Kα radiation, 40 kV and 40 mA, Karlsruhe, Germany). The thermal diffusivity of the samples was measured on a LINSEIS XFA 500 instrument (Linseis Messgeräte GmbH, Selb, Germany) under dynamic vacuum at different temperatures of 30, 60, 90, and 120 °C.

3. Results and Discussion

Figure 1A presents the XRD patterns for the as-prepared Li_3AlH_6 sample. It can be observed that the majority of peaks can be ascribed to Li_3AlH_6, accompanied by a few peaks from impurities of metallic Al. Moreover, the thermal gas desorption properties of the Li_3AlH_6 sample were determined by PCTPRO-2000 and are shown in Figure 1B. A total of 4.63 wt % of hydrogen was liberated from Li_3AlH_6 sample when heated up to 300 °C, which is consistent with the previous studies [7,13]. These results illustrate that Li_3AlH_6 was successfully prepared through ball milling the mixture of $2LiH/LiAlH_4$.

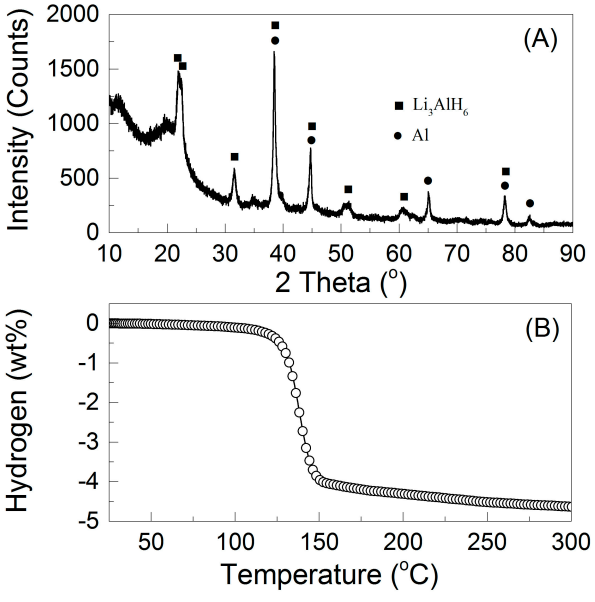

Figure 1. (**A**) XRD pattern and (**B**) Non-isothermal dehydrogenation of the as-prepared Li_3AlH_6 sample.

As shown in Figure 2A, the hydrogen desorption performance of the as-prepared $2LiNH_2$-MgH_2-XLi_3AlH_6 was first evaluated by means of TPD and MS. The operating temperatures for the dehydrogenation of the $2LiNH_2$-MgH_2 system were significantly reduced through the addition of Li_3AlH_6. Interestingly, the dehydrogenation process of the samples with X = 0.05–0.20 exhibited three peaks, which is different from the pristine sample, with only one desorption peak at 184 °C. For the $2LiNH_2$-MgH_2-$0.1Li_3AlH_6$ sample, three dehydrogenation peaks were seen at temperatures of 96, 128, and 180 °C, respectively. A reduction of 52 °C in the first dehydrogenation peak was achieved as compared to the pristine sample of $2LiNH_2$-MgH_2 [32]. MS examination shows that $2LiNH_2$-MgH_2 generated gaseous products including hydrogen and ammonia in a wide heating process. After the addition of Li_3AlH_6, the ammonia emission in the heating process was dramatically suppressed and almost completely inhibited for the sample of $2LiNH_2$-MgH_2-$0.1Li_3AlH_6$.

The hydrogen desorption performance of the as-prepared $2LiNH_2$-MgH_2 samples doped with different amounts of Li_3AlH_6 is shown in Figure 2B. Obviously, the operating temperatures for dehydrogenation were significantly decreased, and the amount of hydrogen released was found to be increased after the addition of Li_3AlH_6. A total of 5.15 wt % of hydrogen was liberated from pristine $2LiNH_2$-MgH_2 when heated up to 300 °C, while 6.47 wt % of hydrogen was released from $2LiNH_2$-MgH_2-0.05 Li_3AlH_6 with an onset temperature of about 102 °C. It is worth noting that the increase of hydrogen capacity for $2LiNH_2$-MgH_2-XLi_3AlH_6 is not proportional to the quantity of Li_3AlH_6 added, implying that Li_3AlH_6 may participate in the dehydrogenation reaction of $2LiNH_2$-MgH_2 during ball milling or heating processes. The onset desorption temperature was found to decrease gradually with an increasing amount of the doped Li_3AlH_6. Considering the hydrogen capacity and the operating temperature, the sample of $2LiNH_2$-MgH_2-$0.1Li_3AlH_6$ exhibited an optimal overall performance in the present study, since it could release 6.43 wt % of hydrogen. Therefore, subsequent investigation of the relationship between hydrogen storage properties and thermal diffusivity was focused on the $2LiNH_2$-MgH_2-$0.1Li_3AlH_6$ sample.

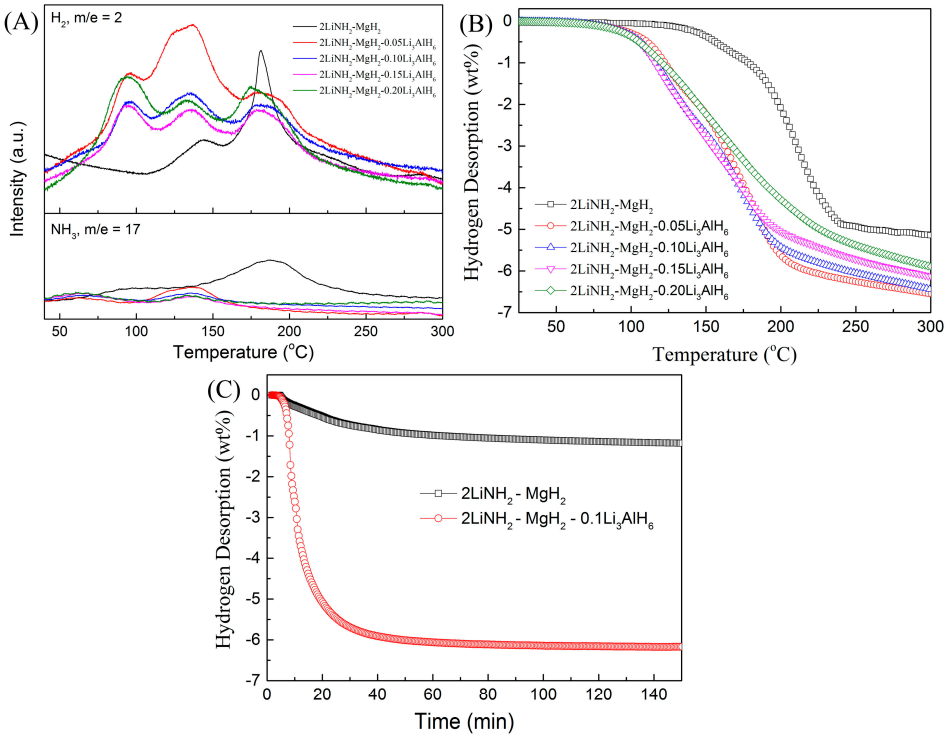

Figure 2. (**A**) Temperature-dependent gas (hydrogen (top) and ammonia (bottom)) released and (**B**) non-isothermal dehydrogenation curves of $2LiNH_2$-MgH_2-XLi_3AlH_6 samples; (**C**) Isothermal dehydrogenation curves of $2LiNH_2$-MgH_2 and $2LiNH_2$-MgH_2-$0.1Li_3AlH_6$ at 160 °C.

The isothermal dehydrogenation curves shown in Figure 2C indicate that the dehydrogenation rate of $2LiNH_2$-MgH_2 was remarkably enhanced by the addition of $0.1Li_3AlH_6$. At 160 °C, about 5.82 wt % of hydrogen was desorbed from $2LiNH_2$-MgH_2-$0.1Li_3AlH_6$ within 30 min, whereas only 0.57 wt % of hydrogen desorbed from $2LiNH_2$-MgH_2. When the dehydrogenation period was extended to 150 min, the amount of hydrogen desorbed from $2LiNH_2$-MgH_2-$0.1Li_3AlH_6$ increased to 6.11 wt %, which is very close to the total hydrogen capacity of 6.43 wt % heated up to 300 °C (Figure 2B). That is to say, the dehydrogenation kinetics was enhanced through the addition of $0.1Li_3AlH_6$, even at low temperature. We performed reversibility tests of the $2LiNH_2$-MgH_2-$0.1Li_3AlH_6$ sample (i.e., rehydrogenation at 200 °C and 50 bar hydrogen pressure). The initial rate for isothermal hydrogen absorption was so quick that the pressure-composition-temperature (PCT) could not accurately record the data. So, the absorption capacity was much lower than the theoretical value, and the hydrogen absorption capacity decreased with the increase of running cycles. Despite all this, it is worth noting that the doped sample had a much better reabsorption property than that of pristine sample.

The study of the dehydrogenation mechanism of the Li-Mg-N-H system shows that poor mass and/or heat transfer for solid–solid reaction is one of the critical issues for altering the thermodynamic and kinetic performance for hydrogen storage [33]. Figure 3 shows the thermal diffusivity of studied samples measured under the same conditions. Obviously, the thermal diffusivity increased after the addition of Li_3AlH_6. Doping with $0.1Li_3AlH_6$ or more gave rise to a significant increase of the thermal diffusivity. The thermal diffusivity of $2LiNH_2$-MgH_2-$0.1Li_3AlH_6$ is about 0.0035 cm^2/s, almost two times higher than that of pristine $2LiNH_2$-MgH_2. With the increase of temperature, the thermal diffusivity of both samples remained roughly constant. As discussed above in this study, the hydrogen storage properties were been significantly improved (i.e., lower dehydrogenation temperature and suppression of the NH_3 evolution after the addition of Li_3AlH_6). It can be concluded that these improvements could be ascribed to the significant increase of thermal diffusivity, helpful to improve the performance of heat transfer for solid–solid reaction, eventually resulting in an enhancement of hydrogen desorption performance.

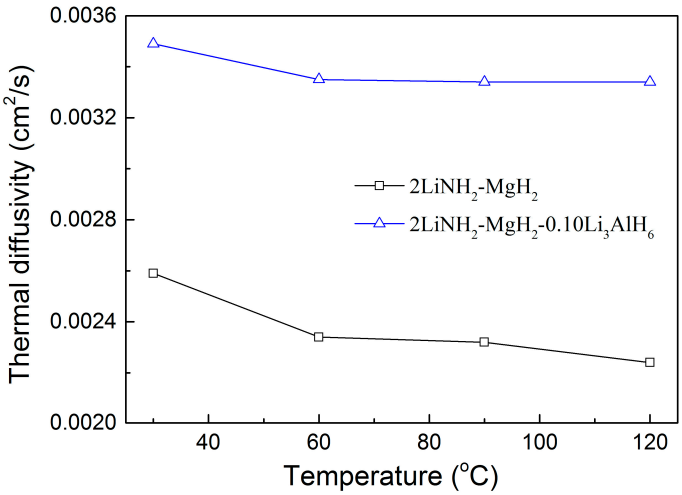

Figure 3. Thermal diffusivity for $2LiNH_2$-MgH_2 and $2LiNH_2$-MgH_2-$0.1Li_3AlH_6$ samples at different temperatures.

On the basis of the results discussed above, it can be deduced that the added Li_3AlH_6 should participate in the dehydrogenation reaction. Therefore, the phase evolution of $2LiNH_2$-MgH_2-$0.1Li_3AlH_6$ during heating process was studied in detail with the XRD patterns shown in Figure 4. It can be observed that in the initial stage, $LiNH_2$ and MgH_2 diffraction peaks were observed for sample after ball milling without detectable Li_3AlH_6, which means that Li_3AlH_6 may transform to an amorphous structure in the process of ball milling. After desorption at 100 °C, about 0.40 wt % of hydrogen was desorbed from $2LiNH_2$-MgH_2-$0.1Li_3AlH_6$, which gives a similar XRD pattern. When heated

to 160 °C, $LiNH_2$ and MgH_2 diffraction peaks almost disappeared. Meanwhile, α-phase $Li_2Mg(NH)_2$ with an orthorhombic structure was formed. Upon further increasing the temperature to 220 °C with about 6.31 wt % of hydrogen released, α-phase $Li_2Mg(NH)_2$ was still the main product. Note that after complete dehydrogenation at 300 °C, β-phase $Li_2Mg(NH)_2$ with a primitive cubic structure was observed, indicating that a solid phase transition of $Li_2Mg(NH)_2$ occurred. The structural transition from an orthorhombic phase to a primitive cubic phase was reported to always occur at an elevated temperature of 400 °C or under a treatment of 36 h of high-energetic ball milling [34]. It should be highlighted that this phase transition occurred below 300 °C in our case, which may be related to the addition of Li_3AlH_6. The study of the underlying mechanism is underway.

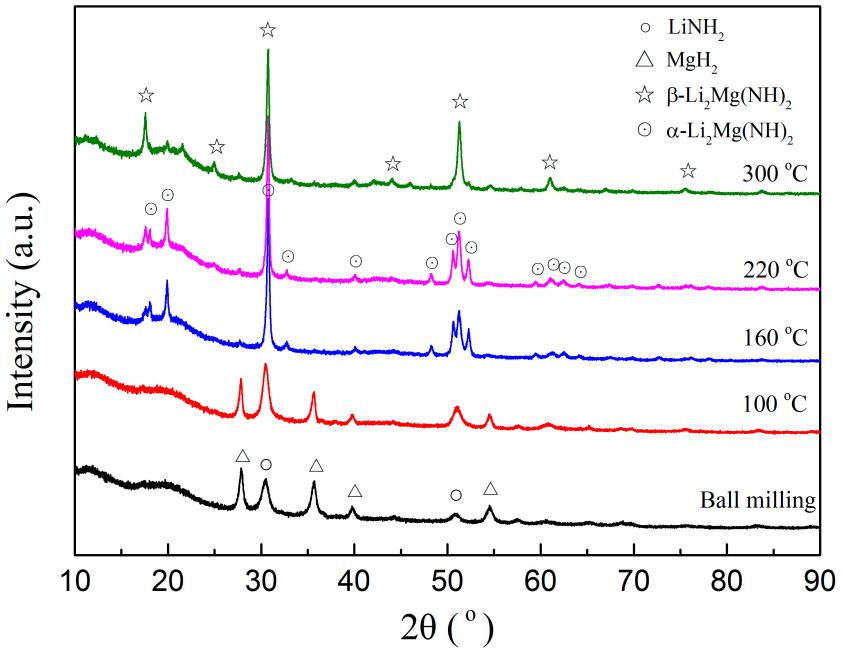

Figure 4. XRD patterns for $2LiNH_2$-MgH_2-$0.1Li_3AlH_6$ sample at different stages.

4. Conclusions

Li_3AlH_6 was prepared by ball milling the mixture of $2LiH/LiAlH_4$. Then, it was doped into $2LiNH_2$-MgH_2, which resulted in an improvement of the dehydrogenation properties. The addition of Li_3AlH_6 not only reduced the dehydrogenation temperatures and increased the amount of hydrogen released from the $2LiNH_2$-MgH_2 system, but also inhibited the release of ammonia as byproduct. $2LiNH_2$-MgH_2-$0.1Li_3AlH_6$ had a reduced onset dehydrogenation temperature of 78 °C without detectable ammonia emission during the whole heating process. Moreover, $2LiNH_2$-MgH_2-$0.1Li_3AlH_6$ had excellent low temperature hydrogen releasing performance (i.e., 6.11 wt % of hydrogen released at 160 °C in 150 min). Moreover, the kinetics for hydrogen reabsorption of $2LiNH_2$-MgH_2-$0.1Li_3AlH_6$ was much better than that of pristine sample, which needs to be confirmed by non-isothermal absorption tests in the future. Doping with $0.1Li_3AlH_6$ gave rise to a high thermal diffusivity, almost two times higher than that of $2LiNH_2$-MgH_2, probably contributing to the improved hydrogen storage properties.

Acknowledgments: This research was financially supported by NSFC (51401059, 51361006, 51461010, 51361005, 51371060, U1501242, and 51461011), the Innovation Project of GUET Graduate Education (2016YJCX22) and GXNSF (2014GXNSFAA118043 and 2014GXNSFAA118333).

Author Contributions: H.C., F.X. and L.S. conceived and designed the experiments; S.Q., X.M. and E.W. performed the experiments; S.Q., Y.Z. and H.C. analyzed the data; S.Q., X.M. and C.X. contributed reagents/materials/analysis tools; S.Q., X.M. and H.C. wrote the paper.

Conflicts of Interest: The authors declare no conflict of interest.

References

1. Meeks, N.D.; Baxley, S. Fuel cells and the hydrogen economy. *Chem. Eng. Prog.* **2016**, *112*, 34–38.
2. Graetz, J. New approaches to hydrogen storage. *Chem. Soc. Rev.* **2009**, *38*, 73–82. [CrossRef] [PubMed]
3. Thomas, K.M. Hydrogen adsorption and storage on porous materials. *Catal. Today* **2007**, *120*, 389–398. [CrossRef]
4. Schuth, F.; Bogdanovic, B.; Felderhoff, M. Light metal hydrides and complex hydrides for hydrogen storage. *Chem. Commun.* **2004**, *20*, 2249–2258. [CrossRef] [PubMed]
5. Orimo, S.I.; Nakamori, Y.; Eliseo, J.R.; Zuttel, A.; Jensen, C.M. Complex hydrides for hydrogen storage. *Chem. Rev.* **2007**, *107*, 4111–4132. [CrossRef] [PubMed]
6. Xiong, Z.T.; Wu, G.T.; Hu, J.J.; Chen, P. Ternary imides for hydrogen strogen. *Adv. Mater.* **2004**, *16*, 1522–1525. [CrossRef]
7. Xiong, Z.T.; Wu, G.T.; Hu, J.J.; Chen, P. Investigation on chemical reaction between $LiAlH_4$ and $LiNH_2$. *J. Power Sources* **2006**, *159*, 167–170. [CrossRef]
8. Wang, H.; Cao, H.J.; Wu, G.T.; He, T.; Chen, P. The improved hydrogen storage performances of the multi-component composite: $2Mg(NH_2)_{2–3}LiH$-$LiBH_4$. *Energies* **2015**, *8*, 6898–6909. [CrossRef]
9. Lu, J.; Fang, Z.Z. Dehydrogenation of a Combined $LiAlH_4/LiNH_2$ System. *J. Phys. Chem. B* **2005**, *109*, 20830–20834. [CrossRef] [PubMed]
10. Wei, J.; Leng, H.Y.; Li, Q.; Chou, K.C. Improved hydrogen storage properties of $LiBH_4$ doped Li-N-H system. *Int. J. Hydrog. Energy* **2014**, *39*, 13609–13615. [CrossRef]
11. Cao, H.J.; Chua, Y.S.; Zhang, Y.; Xiong, Z.T.; Wu, G.T.; Qiu, J.S.; Chen, P. Releasing 9.6 wt % of H_2 from $Mg(NH_2)_{2–3}LiH$-NH_3BH_3 through mechanochemical reaction. *Int. J. Hydrog. Energy* **2013**, *38*, 10446–10452. [CrossRef]
12. Kwak, Y.J.; Kwon, S.N.; Song, M.Y. Preparation of $Zn(BH_4)_2$ and diborane and hydrogen release properties of $Zn(BH_4)_2 + xMgH_2$ (x = 1, 5, 10, and 15). *Met. Mater. Int.* **2015**, *21*, 971–976. [CrossRef]
13. Chen, J.; Kuriyama, N.; Xu, Q.; Takeshita, H.T.; Sakai, T. Reversible hydrogen storage via titanium-catalyzed $LiAlH_4$ and Li_3AlH_6. *J. Phys. Chem. B* **2001**, *105*, 11214–11220. [CrossRef]
14. Chu, H.L.; Xiong, Z.T.; Wu, G.T.; He, T.; Wu, C.Z.; Chen, P. Hydrogen storage properties of Li–Ca–N–H system with different molar ratios of $LiNH_2/CaH_2$. *Int. J. Hydrog. Energy* **2010**, *35*, 8317–8321. [CrossRef]
15. Chua, Y.S.; Chen, P.; Wu, G.T.; Xiong, Z.T. Development of amidoboranes for hydrogen storage. *Chem. Commun.* **2011**, *47*, 5116–5129. [CrossRef] [PubMed]
16. David, W.I.F. Effective hydrogen storage: A strategic chemistry challenge. *Faraday Discuss.* **2011**, *151*, 399–414. [CrossRef] [PubMed]
17. Chen, P.; Zhu, M. Recent progress in hydrogen storage. *Mater. Today* **2008**, *11*, 36–43. [CrossRef]
18. Chen, P.; Xiong, Z.T.; Luo, J.Z.; Lin, J.Y.; Tan, K.L. Interaction of hydrogen with metal nitrides and imides. *Nature* **2002**, *420*, 302–304. [CrossRef] [PubMed]
19. Luo, W.F. ($LiNH_2$-MgH_2): A viable hydrogen storage system. *J. Alloys Compd.* **2004**, *381*, 284–287. [CrossRef]
20. Amica, G.; Larochette, P.A.; Gennari, F.C. Hydrogen storage properties of $LiNH_2$-LiH system with MgH_2, CaH_2 and TiH_2 added. *Int. J. Hydrog. Energy* **2015**, *40*, 9335–9346. [CrossRef]
21. Li, Y.T.; Ding, X.L.; Wu, F.L.; Sun, D.L.; Zhang, Q.A.; Fang, F. Enhancement of hydrogen storage in destabilized $LiNH_2$ with $KMgH_3$ by quick conveyance of N-containing species. *J. Phys. Chem. C* **2016**, *120*, 1415–1420. [CrossRef]
22. Shukla, V.; Bhatnagar, A.; Pandey, S.K.; Shahi, R.R.; Yadav, T.P.; Shaz, M.A.; Srivastava, O.N. On the synthesis, characterization and hydrogen storage behavior of $ZrFe_2$ catalyzed Li-Mg-N-H hydrogen storage material. *Int. J. Hydrog. Energy* **2015**, *40*, 12294–12302. [CrossRef]
23. Principi, G.; Agresti, F.; Maddalena, A.; Russo, S. The problem of solid state hydrogen storage. *Energy* **2009**, *34*, 2087–2091. [CrossRef]
24. Nakamori, Y.; Ninomiya, A.; Kitahara, G.; Aoki, M.; Noritake, T.; Miwa, K.; Kojima, Y.; Orimo, S. Dehydriding reactions of mixed complex hydrides. *J. Power Sources* **2006**, *155*, 447–455. [CrossRef]
25. Ono, T.; Shimoda, K.; Tsubota, M.; Kohara, S.; Ichikawa, T.; Kojima, K.; Tansho, M.; Shimizu, T.; Kojima, Y. Ammonia desorption property and structural changes of $LiAl(NH_2)_4$ on thermal decomposition. *J. Phys. Chem. C* **2011**, *115*, 10284–10291. [CrossRef]

26. Siangsai, A.; Suttisawat, Y.; Sridechprasat, P.; Rangsunvigit, P.; Kitiyanan, B.; Kulprathipanja, S. Effect of Ti compounds on hydrogen desorption/absorption of $LiNH_2/LiAlH_2/MgH_2$. *J. Chem. Eng. Jpn.* **2008**, *43*, 95–98. [CrossRef]
27. Andreasen, A.; Vegge, T.; Pedersen, A.S. Dehydrogenation kinetics of as-received and ball-milled $LiAlH_4$. *J. Solid State Chem.* **2005**, *178*, 3672–3678. [CrossRef]
28. Andreasen, A. Effect of Ti-doping on the dehydrogenation kinetic parameters of lithium aluminum hydride. *J. Alloys Compd.* **2006**, *419*, 40–44. [CrossRef]
29. Lu, J.; Fang, Z.Z.; Sohn, H.Y.; Bowman, R.C.; Hwang, S.J. Potential and reaction mechanism of Li-Mg-Al-N-H system for reversible hydrogen storage. *J. Phys. Chem. C* **2007**, *111*, 16686–16692. [CrossRef]
30. Xiong, Z.T.; Wu, G.T.; Hu, J.J.; Liu, Y.F.; Chen, P.; Luo, W.F.; Wang, J. Reversible hydrogen storage by a Li-Al-N-H complex. *Adv. Funct. Mater.* **2007**, *17*, 1137–1142. [CrossRef]
31. Lu, J.; Fang, Z.Z.; Sohn, H.Y. A new Li-Al-N-H system for reversible hydrogen storage. *J. Phys. Chem. B* **2006**, *110*, 14236–14239. [CrossRef] [PubMed]
32. Wang, J.H.; Liu, T.; Wu, G.T.; Li, W.; Liu, Y.F.; Araujo, C.M.; Scheicher, R.H.; Blomqvist, A.; Ahuja, R.; Xiong, Z.T.; et al. Potassium-modified $Mg(NH_2)_2/2LiH$ system for hydrogen storage. *Angew. Chem. Int. Ed.* **2009**, *48*, 5828–5832. [CrossRef] [PubMed]
33. Chen, P.; Xiong, Z.T.; Yang, L.F.; Wu, G.T.; Luo, W.F. Mechanistic investigations on the heterogeneous solid-state reaction of magnesium amides and lithium hydrides. *J. Phys. Chem. B* **2006**, *110*, 14221–14225. [CrossRef] [PubMed]
34. Liang, C.; Gao, M.X.; Pan, H.G.; Liu, Y.F. Structural transitions of ternary imide $Li_2Mg(NH)_2$ for hydrogen storage. *Appl. Phys. Lett.* **2014**, *105*, 083909. [CrossRef]